Building and Environment 45 (2010) 2545–2552

Contents lists available at ScienceDirect

Building and Environment

journal homepage: www.elsevier.com/locate/buildenv

Numerical simulation of radiant floor cooling system: The effects of thermal resistance of pipe and water velocity on the performance

Xing Jin*, Xiaosong Zhang, Yajun Luo, Rongquan Cao

School of Energy and Environment, Southeast University, Nanjing 210096, PR China

ARTICLE INFO

Article history:
Received 20 January 2010
Received in revised form
12 May 2010
Accepted 14 May 2010

Keywords:
Radiant floor cooling
Composite grid
Finite volume method
Numerical simulation

ABSTRACT

Using the existing floor heating system, the radiant floor cooling system can be used as an alternative to the conventional all-air cooling systems. In this paper, a numerical model for the radiant floor cooling system is built using finite volume method. The objective of this study is to research the effects of the thermal resistance of pipe and water velocity on the performance of the radiant floor cooling system. In order to provide better heat transfer simulation in the pipe, composite grids are used in the model. The numerical floor surface temperature and the heat flux are in agreement with the measured results. The results illustrate that the pipe has effect on the performance of the radiant floor cooling system when the thermal conductivity of the pipe is low. However, the effect of the water velocity on the performance of the cooling system is not great. The model is helpful to calculate and design such kind of radiant floor cooling systems.

1. Introduction

The radiant floor heating system has been widely used in many countries for its energy savings, comfort and health. While in summer, many of these areas also need cooling system. If the radiant floor heating system is used to supply cooing in summer, the initial cost of the system will be saved and the utilization ratio of the devices will increase [1,2].

Compared to the conventional air-conditioning, the recently researches show that the radiant cooling system can save energy consumption and create a more comfortable environment [1,3–6]. In addition, because the radiant cooling system is a high-temperature cooling system, it enables a higher efficiency for a chiller. As the ground temperature is often around 10 °C, it is also possible to cool a floor directly from a ground heat exchanger (pipes embedded in the ground or foundation) without the use of a chiller [7]. Meanwhile, the angle factor for person in floor cooling system is about as 2.5 times as that in ceiling cooling system, which means one degree change of the floor temperature will have 2.5 times the effect on the mean radiant temperature than one degree change of the ceiling temperature [8].

Because the radiant floor system can be used to provide both heating and cooling, the numerical model of radiant cooling is almost the same as the model of radiant heating. There have been many studies on the mathematic model of radiant floor heating in the literature. Ho et al. [9] built the numerical models of floor heating system by the finite difference method and the finite element method, respectively. Of the two, the finite difference method gave slightly higher temperature values and required more execution time. Steady state results from the simulation compared well with the experimental results. Sattari and Farhanieh [10] studied the effects of design parameters on performance of a typical radiant floor heating system using finite element method. It was noted that the type and thickness of the floor cover material were the most important parameters in the design of radiant heating systems. Song [11] studied the performance of the ONDOL floor heating system with 10 types of covering materials by experiment. The results showed that the lower the contact coefficient of covering material, the more stable the temperature fluctuation in the floor surface was. Holopainen et al. [12] built the simulation model of floor heating system using an uneven nodal network. The results showed that the uneven gridding method was more profitable with the homogenous floor case, and the simulation times were shorter. Laouadi [13] built a model which combined the one-dimensional numerical model of the energy simulation software with a two-dimensional analytical model. The model predictions for slab-on-grade heating systems compared very well with the results from a full two-dimensional numerical model.

However, in the literature, the thermal resistance of the pipe is neglected, and the water flow is assumed to be turbulent. In many

* Corresponding author. Tel./fax: +86 25 83792722.
E-mail address: jxining@163.com (X. Jin).

0360-1323/$ – see front matter © 2010 Elsevier Ltd. All rights reserved.
doi:10.1016/j.buildenv.2010.05.016

Nomenclature

D	diameter (m)
F	area (m^2)
Gr	Grashof number
h	heat transfer coefficient [W/(m^2 K)]
L	characteristic length (m)
Pr	Prandtl number
q	heat flux (W/ m^2)
Re	Reynolds number
S	pipe spacing (mm)
t	temperature (°C)
T	temperature (K)
W	width of the nozzle opening (m)
v	velocity (m/s)
X	angle factor

Greek symbols

ε	emissivity
λ	thermal conductivity [W/(m K)]
σ	Boltzmann constant [W/(m^2 K^4)]
δ	thickness (mm)
Φ	heat transfer rate (W)

Subscripts

a	air
av	average
b	bottom
c	convective
fc	forced convection
i	inner
mc	mixed convection
nc	natural convection
os	room other surfaces (walls and ceiling)
p	pipe
r	radiant
s	floor surface
w	water

floor heating/cooling systems, the pipe is made of plastic, the thermal resistance of which is high, and the convective heat transfer coefficient between the water and pipe is more than the heat conduction coefficient of the floor material even though the flow is laminar. Therefore, the influences of the pipe and water velocity on the performance of the system need to be studied more.

In this paper, a finite volume model is constructed for the radiant floor cooling system. The effect of the pipe thermal resistance and water velocity on the performance of the system will be researched. In general, the pipe used in the radiant floor system is cylinder in shape, while the floor layers are cuboids in shape. In the simulation, the rectangular coordinate system can be used in the floor layers, but it cannot be used in the pipes. Therefore, for providing better heat transfer simulation in the pipe, composite grids are used in the model. The rectangular coordinate system is used in the floor layers. However, the cylindrical coordinate system is used in the pipe for the 3-D simulation, the polar coordinate system is used in the pipe for the 2-D simulation. Composite grids have been used to solve many problems efficiently and accurately, such as flow, combustion, heat transfer, aerodynamics [14–19], etc.

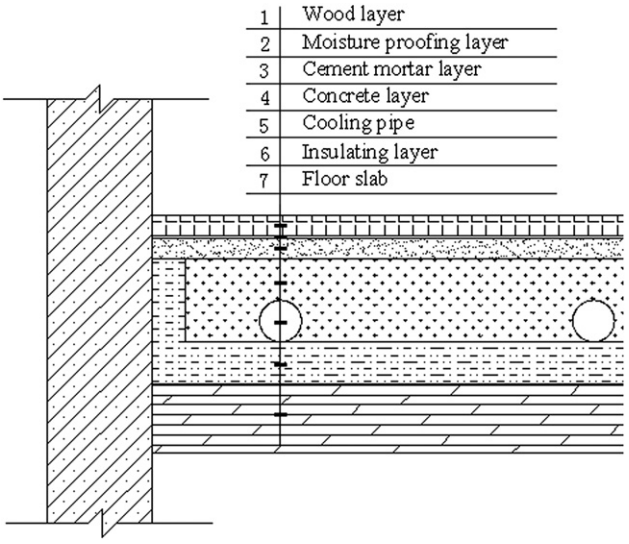

Fig. 1. The floor physical model.

However, to our knowledge, the present work is the first application of composite grids to the floor heating/cooling system.

2. Methodology

2.1. Physical model

In this study, the physical model of the floor is based on an experimental house, which is located in Southeast University, Nanjing, China. The structure of the floor is shown in Fig. 1. In some other houses, the surface layer may be the tile or there are not cement mortar layer and moisture proofing layer. The material properties used in the floor layer are shown in Table 1. In the study, the spacing between two pipes is 150 mm, the inner diameter of the pipe is 16 mm.

The configuration of the pipes in the radiant floor cooling system is shown in Fig. 2. The advantage of the configuration is the high and low temperature pipes alternate with each other, the floor surface temperature is uniform and the pipes do not intersect with each other. The average temperature of the supply and return water is used as the calculated water temperature in this paper.

2.2. Meshing

The three-dimensional heat transfer in the floor is complicated. In fact, the water temperature changes slowly along with the pipe, so the heat transfer in the floor can be simplified to the two-dimensional heat transfer.

The whole floor layer is divided into 5 sub-domains, as shown in Fig. 3. I is the surface layer, II is the moisture proofing layer, III contains cement mortar layer, concrete layer and insulating layer, IV and V are the PPR-pipes. The rectangular coordinate system is

Table 1
The thermal conductivity of material.

Structural layers	Thermal conductivity λ [W/(m K)]	Thickness δ(mm)
Wood layer	0.14	10
Tile layer	1.1	10
Moisture proofing layer	0.03	1
Cement mortar layer	0.93	10
Concrete layer	1.28	40
PPR-pipe	0.22	2
Insulating layer	0.035	20

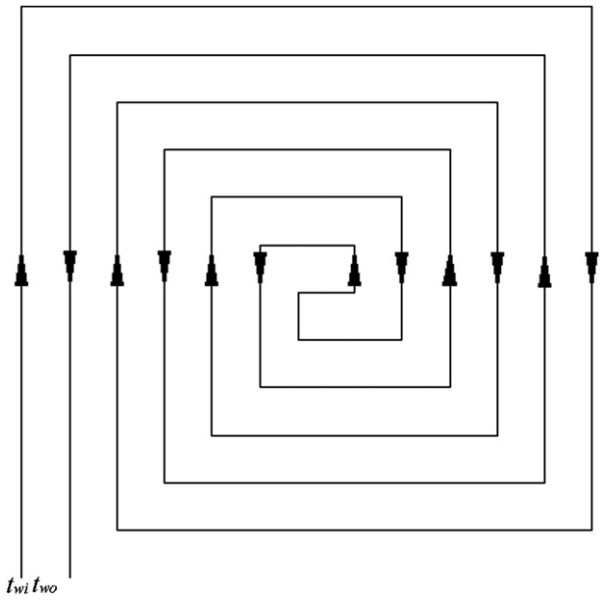

Fig. 2. The configuration of pipes.

used in I, II, III, while the polar coordinate system is used in IV and V. Considering the accuracy and operation speed of the calculation, the size of the grid in I and III is 2 mm × 2 mm. Because the thickness of II is 1 mm, the size of the grid is 2 mm × 1 mm. Fig. 4 shows the composite grids in III, IV and V.

2.3. Governing equations and boundary conditions

In order to simplify the model of heat transfer, the following assumptions are applied

(1) The vertical central planes of the pipes are assumed to be adiabatic because of the symmetry of the temperature;
(2) Because the thermal conductivity of the insulating layer is very low, the temperature differences are very small among the bottom surface of the insulating layer. In this study, the temperature of the bottom surface of the insulating layer is assumed to be uniform;
(3) All the materials are assumed to be isotropic mediums.

Governing equations for the floor:

$$\frac{\partial^2 t}{\partial x^2}+\frac{\partial^2 t}{\partial y^2} = 0, (x, y\in \mathrm{I, II, III}) \tag{1}$$

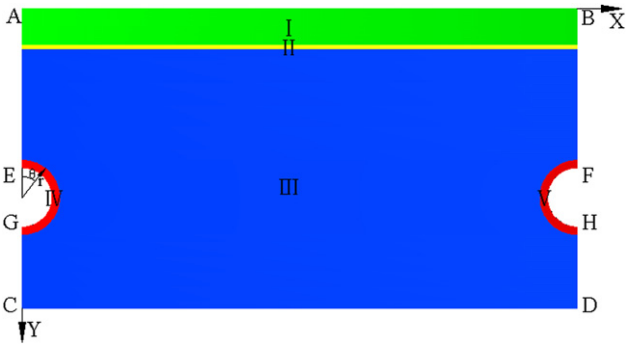

Fig. 3. Sub-domains of the floor.

$$\frac{\partial^2 t}{\partial r^2}+\frac{1}{r^2}\frac{\partial^2 t}{\partial \theta^2} = 0, (r, \theta\in \mathrm{IV, V}) \tag{2}$$

The boundary conditions of the governing equations are

$$\frac{\partial t}{\partial x} = 0(x, y\in \mathrm{AE, GC, BF, HD}) \tag{3}$$

$$t = t_b, (x, y\in \mathrm{CD}) \tag{4}$$

$$\lambda_s\frac{\partial t}{\partial y} = h_s(t-t_a), (x, y\in AB) \tag{5}$$

$$\lambda_p\frac{\partial t}{\partial r} = h_w(t-t_w), (x, y\in \mathrm{EG, FH}) \tag{6}$$

The floor surface average temperature is calculated by equation (7).

$$t_s = \frac{1}{S}\int_0^S t_{i0}\mathrm{d}x \tag{7}$$

where t_b, t_a, t_w are the temperature of the bottom surface of the insulating layer, the air and the water, respectively. λ_s, λ_p are the thermal conductivity of the surface layer and the pipe, respectively.

2.4. Heat transfer in floor cooling system

2.4.1. Radiant heat flux

The room surface is assumed as a closed-system consisted of two gray surfaces which are the floor surface and room other surfaces (walls and ceiling), respectively. The radiant heat flux between two gray surfaces can be calculated by the following equations:

$$q_r = \frac{\sigma\left(T_{\mathrm{os}}^4 - T_s^4\right)}{\left(\frac{1}{\varepsilon_1}-1\right)+\frac{1}{X_{12}}+\frac{F_1}{\sum_2^6 F_i\left(\frac{1}{\varepsilon_2}-1\right)}} \tag{8}$$

$$T_{\mathrm{os}} = \frac{\sum_{i=2}^6 (F_i T_i)}{\sum_{i=2}^6 F_i} \tag{9}$$

where q_r is radiant heat flux, T_s is the floor surface temperature, T_{os} is the average temperature of room other surfaces, F_1 is the floor area, F_i is room other surfaces area.

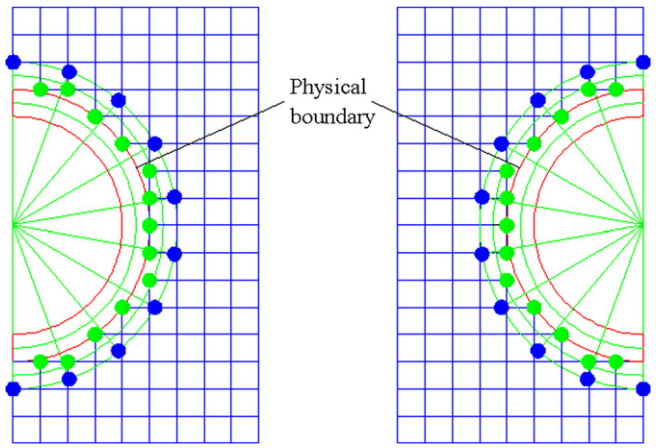

Fig. 4. The composite grids in III, IV and V.

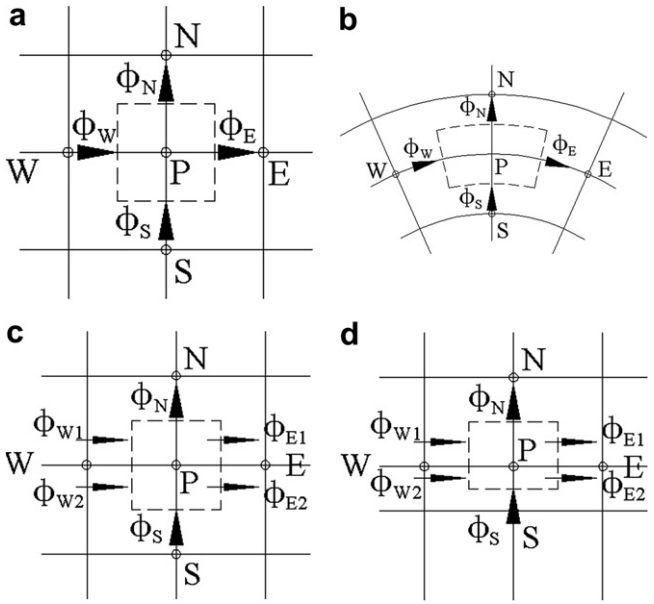

Fig. 5. The diagram of nodes (a) node in rectangular coordinate system, (b) node in polar coordinate system, (c) node in the interface of the two materials, (d) node in the moisture proofing layer.

The radiant heat transfer coefficient between the floor and the room other surfaces is presented in equation (10).

$$h_r = \frac{q_r}{T_{os} - T_s} \tag{10}$$

where h_r is radiant heat transfer coefficient between the floor and the room other surfaces.

2.4.2. Convective heat flux between the floor and the air

The convective heat flux between the floor and the air is presented in equation (11).

$$q_c = h_c(t_a - t_s) \tag{11}$$

where q_c is convective heat flux, h_c is the convective heat transfer coefficient between the floor and the air.

In the case of natural convection, the convective heat transfer coefficient for heated ceiling or cooled floor can be calculated by equation (12) [22].

$$h_{nc} = 0.27\frac{\lambda_a}{L}(Gr\mathrm{Pr})^{0.25} \tag{12}$$

where h_{nc} is natural convective heat transfer coefficient, λ_a is the air thermal conductivity.

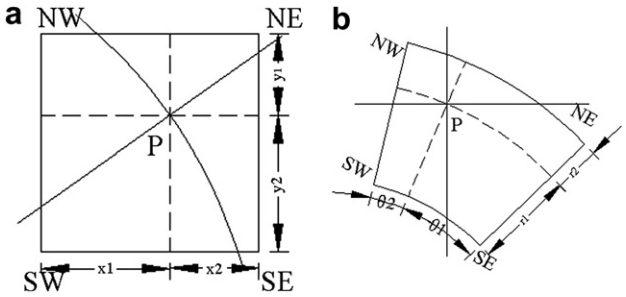

Fig. 6. The composite grid in concrete and pipes (a) node in rectangular coordinate system, (b) node in polar coordinate system.

In the case of mixed convection, Neiswanger et al. [20] postulated that the convective heat transfer coefficient could be presented in terms of the limiting cases of forced and natural convection, as follow:

$$h_{mc} = \left(h_{nc}^{3.2} + h_{nc}^{3.2}\right)^{1/3.2} \tag{13}$$

where h_{mc} is the mixed convective heat transfer coefficient and h_{fc} is forced convective heat transfer coefficient.

They also proposed that the h_{fc} could be correlated in terms of Reynolds number alone. Awbi [21] studied the mixed convective heat transfer for walls, floor and ceiling. The experimental data of supply air from lower part indicated h_{fc} could be calculated by equation (14).

$$h_{fc} = 4.248W^{0.575}v^{0.557} \tag{14}$$

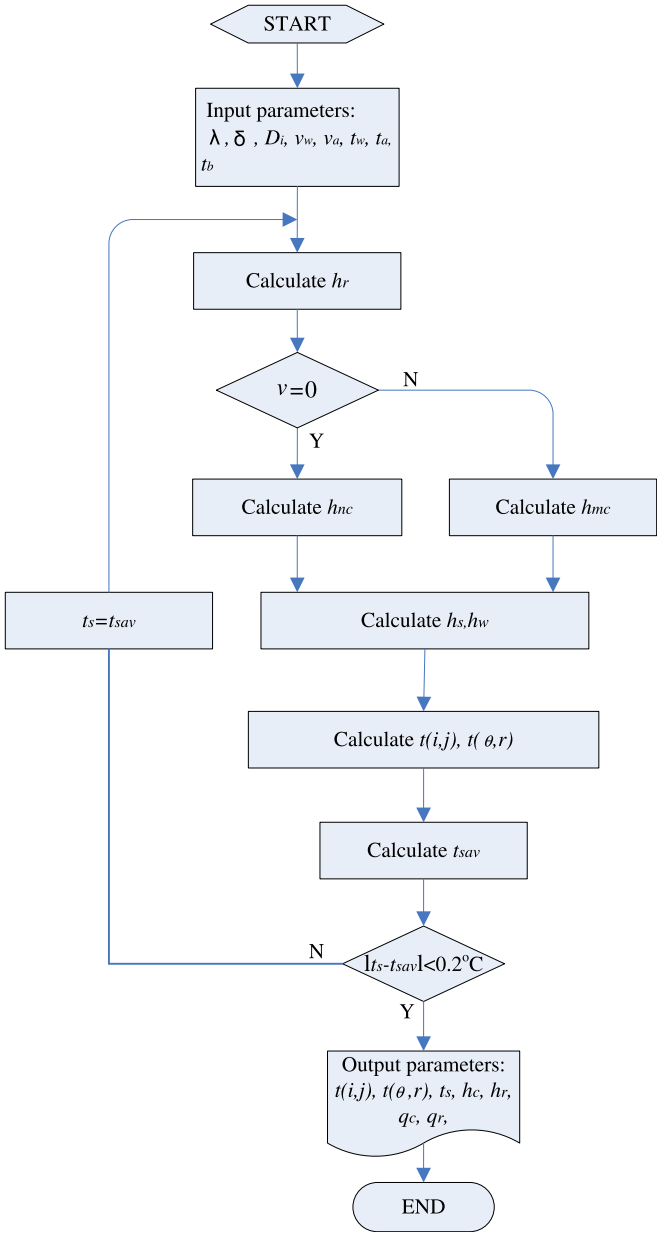

Fig. 7. Scheme of computer design.

Table 2
Comparison of numerical and measured floor surface temperature under the same water velocity.

Average temperature of walls and ceiling t_{os} (°C)	Air temperature t_a (°C)	Water temperature t_w (°C)	Water velocity v_w (m/s)	Floor surface temperature t_f (°C)			Absolute error between measured value and numerical value with pipe (°C)
				Measured	Numerical		
					Without pipe	With pipe	
28.3	27.2	10.8	0.666	20.7	19.78	20.43	0.26
28.6	27.5	11.9	0.666	21.2	20.44	21.07	0.13
28.5	27.4	13.8	0.666	21.9	21.31	21.82	0.08
26.7	25.7	13.8	0.666	21.1	20.34	20.81	0.29
27.5	26.4	15.8	0.666	22.4	21.70	22.10	0.30
25.7	24.7	16.8	0.666	21.8	21.21	21.50	0.30
26.2	25.3	18.2	0.666	22.7	22.15	22.41	0.29
26.7	25.8	20.2	0.666	23.8	23.35	23.51	0.29

2.4.3. Convective heat transfer coefficient between the water and the pipe

The convective heat transfer coefficient between the water and the pipe can be calculated by the following equations [22].

$$h_w = 0.023\mathrm{Re}^{0.8}\mathrm{Pr}^{0.4}\frac{\lambda_p}{D_i}(\mathrm{Re} \geq 10000) \tag{15}$$

$$h_w = 1.86\left(\mathrm{RePr}\frac{D_i}{L}\right)^{\frac{1}{3}}\frac{\lambda_p}{D_i}\left(\mathrm{Re} < 2200, \mathrm{RePr}\frac{D_i}{L} > 10\right) \tag{16}$$

$$h_w = \left(3.66 + \frac{0.0668\mathrm{RePr}\frac{D_i}{L}}{\left(1 + 0.04\mathrm{RePr}\frac{D_i}{L}\right)^{\frac{2}{3}}}\right)\frac{\lambda_p}{D_i}\left(\mathrm{Re} < 2200, \mathrm{RePr}\frac{D_i}{L} \leq 10\right) \tag{17}$$

$$h_w = 0.116\left(\mathrm{Re}^{\frac{2}{3}} - 125\right)\mathrm{Pr}^{\frac{1}{3}}\left(1 + \left(\frac{D_i}{L}\right)^{\frac{2}{3}}\right)\frac{\lambda_p}{D_i}(2200 \leq \mathrm{Re} < 10000) \tag{18}$$

where, h_w is the convective heat transfer coefficient between the water and the pipe.

2.5. Discrete equations

The equations are discretized by the finite volume method. The finite volume equations are gained by the heat balance of each unit, as shown in Fig. 5 (a, b). The equation (19) is the heat balance equation of each unit.

$$\Phi_W + \Phi_S = \Phi_E + \Phi_N \tag{19}$$

In the interface of the two materials, the heat balance of each unit is different because of the different thermophysical properties, as shown in Fig. 5 (c). The heat balance of the moisture proofing layer is also different because of the size of the grid is smaller, as shown in Fig. 5 (d).

The detail diagram of the composite grid in concrete and pipes is shown in Fig. 6, the value of each node can be calculated by the following equations.

$$t_p = \frac{(t_{\mathrm{NE}}x_1 + t_{\mathrm{NW}}x_2)y_2 + (t_{\mathrm{SE}}x_1 + t_{\mathrm{SW}}x_2)y_1}{(x_1 + x_2)(y_1 + y_2)} \tag{20}$$

$$t_p = \frac{(t_{\mathrm{NW}}r_1 + t_{\mathrm{SW}}r_2)\theta_1 + (t_{\mathrm{NE}}r_1 + t_{\mathrm{SE}}r_2)\theta_2}{(r_1 + r_2)(\theta_1 + \theta_2)} \tag{21}$$

2.6. Solving the model

The numerical simulation model is illustrated in Fig. 7. The initial temperatures of all the nodes are set to be equal to the water temperature. According to the measured values in the experiments, the temperature of the bottom surface of the insulating layer is assumed to be 16.5 °C. And then the radiant heat transfer coefficient

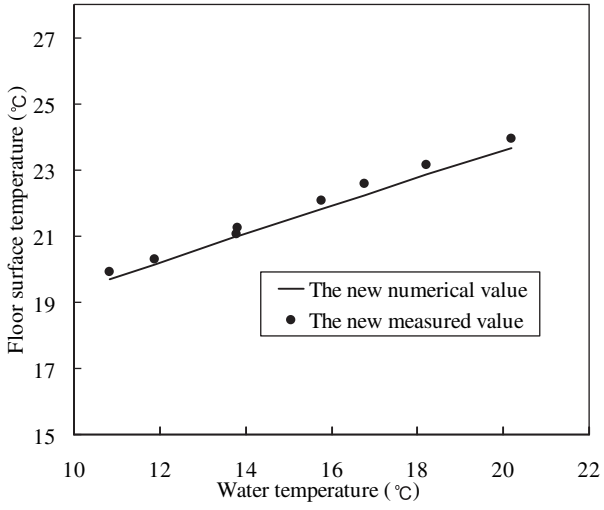

Fig. 8. Comparison of the new numerical and measured floor surface temperature under the same water velocity.

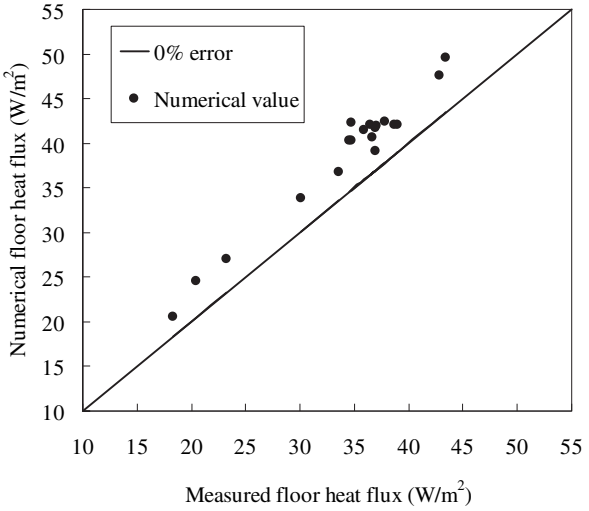

Fig. 9. Comparison of the numerical and measured floor heat flux.

Table 3
The effect of the thermal conductivity of pipe on the floor surface temperature.

Thermal conductivity λ_p [W/(m K)]	0.22	0.50	1.00	100.00	397.00	$+\infty$
Floor surface temperature t_f (°C)	20.27	19.92	19.75	19.55	19.54	19.53

(h_r) and the convective heat transfer coefficients (h_c, h_w) are calculated. The nodes temperatures are gained by Gauss Seidel iteration, the maximum difference between successive elements of the solution is less than 10^{-6}. The floor surface average temperature is the most important parameter in the model. It affects the cooling capacity of the radiant floor cooling system. Therefore, the floor surface average temperature is used to judge the convergence of the model.

The model also can be used to simulate the system in different floor material, different floor layer thickness or different pipe spacing just by changing the input parameters.

3. Validation of the model

Experiments of a kind of such floor cooling system were carried out in an house in May 2009. The dimensions of the house are 4 m (length) × 3 m (width) × 3 m (height). The roof and walls were made of 100-mm-thick polystyrene wrapped by metal board. The structure of the floor is the same as the model. A water-chiller is used to provide cold water to the pipes in the floor. The heat source in the house is simulated by several incandescent lamps, the power of which is measured by the power meter. There are 9 thermocouples on the floor, 3 thermocouples on the inside surface of each wall and ceiling, 3 thermocouples in the indoor air, 3 thermocouples on the outside surface of the walls, and 2 resistance thermometers in the outdoor air. The inlet and outlet temperature and the flow rate of the cold water are measured by the thermocouples and turbine flow meter, respectively.

4. Results and discussions

4.1. Comparison of the numerical and measured floor surface temperature

Table 2 shows the comparison of the numerical and measured values. As shown in the Table, the numerical values are very close to the measured values, the absolute error is less than 0.3 °C.

As the average temperature of walls and ceiling and the air temperature are both different in each experiment, the effect of the water temperature on the floor surface temperature cannot be obtained directly. Therefore, the experimental conditions are set to be the same conditions in this study. Firstly, the average temperature of walls and ceiling and the air temperature are set to be 27 °C and 26 °C, respectively, which are close to the experimental values; Secondly, the new numerical values of floor surface temperature are obtained in the setting conditions by using the model; Thirdly, the temperature difference between the new and original numerical values is calculated; Fourthly, the new measured values are obtained by adding the temperature difference to the original measured values. Fig. 8 presents the new numerical and measured values. As shown in this figure, the numerical values are close to the measured values, too. There is a linear relationship between the water temperature and the floor surface temperature.

4.2. Comparison of the numerical and measured floor heat flux

Fig. 9 shows the numerical and measured values of the floor heat flux. As shown in this figure, the numerical values are a little more than the measured values. In the model, the floor surface temperatures are about 0.4 °C less than measured values (as shown in Table 2 and Table 4), if the actual floor surface temperature is input to the model to calculate the heat flux, the numerical heat flux will decrease by 2.5 W. The numerical and measured values will be much closer.

4.3. Effect of the thermal resistance of pipe on the floor surface temperature

As shown in Table 2, the numerical floor surface temperature with pipe is about 0.4 °C more than the temperature without pipe. It means the temperature error is 0.4 °C if the thermal resistance of pipe is neglected. The water temperature is lower, the temperature error is larger.

In some systems, the thermal resistance of all the layers is lower than that in the model. Assume the floor surface average temperatures are all the same in the different systems. It means the supply water temperature is higher if the thermal resistance of all layers in the system is lower. The efficiency of the chiller will be improved because of the higher supply water temperature. Therefore, a new floor cooling system which has lower thermal resistance is chosen to discuss below. The system does not have the cement mortar layer and moisture proofing layer, the surface layer is tile, while other parameters are the same with the system discussed above. The average temperature of walls and ceiling, the air temperature and the water temperature are set to be 27 °C, 26 °C and 17 °C, respectively. The effect of the thermal resistance of pipe on the floor surface temperature is shown in Table 3. As shown in this Table, if the thermal resistance of the pipe is neglected, the temperature error will be 0.74 °C when the thermal conductivity is 0.22 W/(m K). If the pipe is made of copper or aluminum, the thermal conductivities of which are more than 100 W/(m K), the error is very small.

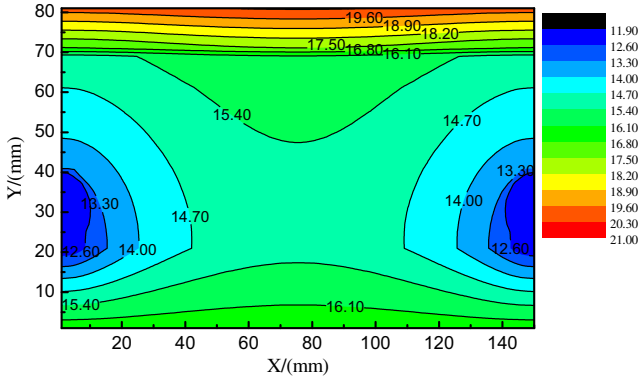

Fig. 10. Isothermal of the floor (t_w = 11.9 °C).

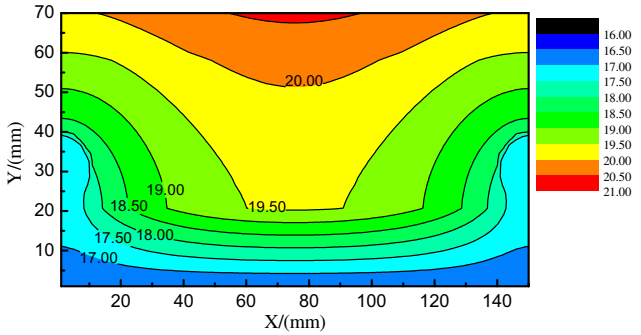

Fig. 11. Isothermal of the floor (t_w = 17 °C).

Table 4
Comparison of numerical and measured floor surface temperature under different water velocity.

Average temperature of walls and ceiling t_{os} (°C)	Air temperature t_a (°C)	Water temperature t_w (°C)	Water velocity v_w (m/s)	Floor surface temperature t_f (°C)		Absolute error (°C)
				Measured	Numerical	
25.5	26.6	11.0	0.132	20.2	19.86	0.34
25.2	26.3	11.2	0.161	20.1	19.76	0.34
24.9	26.2	11.2	0.223	19.9	19.45	0.45
24.9	26.2	11.1	0.249	19.9	19.39	0.51
25.0	26.2	11.0	0.298	19.9	19.34	0.56
25.3	26.4	11.4	0.329	19.9	19.63	0.27
24.9	26.1	11.3	0.415	19.9	19.39	0.51
24.5	25.8	11.4	0.534	19.7	19.25	0.45
25.1	26.1	11.1	0.666	19.7	19.31	0.39
24.4	25.6	11.2	0.803	19.6	19.05	0.55

4.4. The floor temperature field

The temperature distributions of the floor are shown in Fig. 10 and Fig. 11. The floor structure in Fig. 10 is the same as that in Fig. 8. The floor structure in Fig. 11 is the same as that in Table 3. The average temperature of walls and ceiling, the air temperature, the water velocity and the thermal conductivity of the pipe are both 27 °C, 26 °C, 0.666 m/s and 0.22 W/(m K), respectively. The water temperature in Fig. 10 and Fig. 11 are 11.9 °C and 17 °C, respectively. As shown in the figures, the isothermal lines in wood layer and pipe are more, while in tile layer and concrete layer are less. The floor surface temperature fluctuation of wood is more stable than tile. The results are in agreement with the researches of Sattari et al. [10] and Song [11].

4.5. Effect of the water velocity on the floor surface temperature

The numerical and measured values of floor surface temperature under different water velocity are shown in Table 4. The results show that the numerical values are also close to the measured values. The same as the discussion above, the average temperature of walls and ceiling, the air temperature and the water temperature are set to be 26 °C, 25 °C and 11.2 °C, respectively. The new numerical and measured values are shown in Fig. 12. As shown in this figure, the effect of water velocity on the floor surface temperature is small. The floor surface temperature difference between the laminar flow and turbulent flow is about 0.3 °C. On the same condition with Table 3, the floor surface temperature difference between laminar flow and turbulent flow is about 0.5 °C when the thermal conductivity of pipe is 0.22 W/(m K). It is still not large. It means that the water velocity can be set to be a lower value in the system for reducing the energy consumption of the pump.

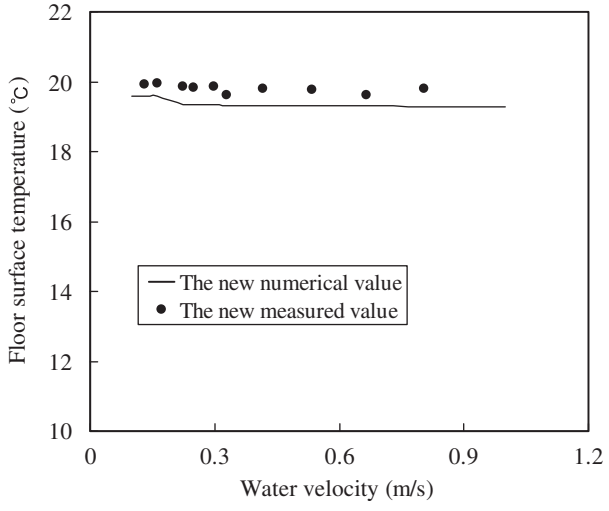

Fig. 12. Comparison of the new numerical and measured floor surface temperature under different water velocity.

5. Conclusions

A numerical model of radiant floor cooling system using finite volume method with composite grids is built in this paper. The numerical model is validated by the experiment. Based on the analysis of the numerical and measured results, the conclusions can be summarized as:

(1) The pipe has effect on the performance of the radiant floor cooling system when the thermal conductivity of the pipe is low.
(2) The effect of the water velocity on the performance of the radiant floor cooling system is not great even though the flow is laminar. Therefore, the energy consumption of the pump can be saved by reducing the water velocity.

Acknowledgments

This research was supported by the 11th Five Year National Science and Technology Support Key Project of China under the Contract No. 2008BAJ12B02 and the Scientific Research Foundation of Graduate School of Southeast University under the Contract No. YBJJ0814.

References

[1] Song D, Kim T, Song S, Hwang S, Leigh SB. Performance evaluation of a radiant floor cooling system integrated with dehumidified ventilation. Applied Thermal Engineering 2008;28:1299–311.
[2] Lim JH, Jo JH, Kim YY, Yeo MS, Kim KW. Application of the control methods for radiant floor cooling system in residential buildings. Building and Environment 2006;41:60–73.
[3] Feustel HE, Stetiu C. Hydronic radiant cooling: preliminary assessment. Energy and Buildings 1995;22:193–205.
[4] Stetiu C. Energy and peak power saving potential of radiant cooling systems in US commercial buildings. Energy and Buildings 1999;30:127–38.
[5] Imanari T, Omori T, Bogaki K. Thermal comfort and energy consumption of the radiant ceiling panel system: comparison with the conventional all-air system. Energy and Buildings 1999;30:167–75.
[6] Niu JL, Zhang LZ, Zuo HG. Energy savings potential of chilled ceiling combined with desiccant cooling in hot and humid climates. Energy and Buildings 2002;34:487–95.
[7] Olesen BW. Radiant floor heating in theory and practice. ASHRAE Journal 2002;44(7):19–24.
[8] Olesen BW. Possibilities and limitations of radiant floor cooling. ASHRAE Transaction 1997;103(1):42–8.
[9] Ho SY, Hayes RE, Wood RK. Simulation of the dynamic behaviour of a hydronic floor heating system. Heat Recovery Systems and CHP 1995;15(6):505–19.
[10] Sattari S, Farhanieh B. A parametric study on radiant floor heating system performance. Renewable Energy 2006;31:1617–26.

[11] Song GS. Buttock responses to contact with finishing materials over the ONDOL floor heating system in Korea. Energy and Buildings 2005;37:65–75.
[12] Holopainen R, Tuomaala P, Piippo J. Uneven gridding of thermal nodal networks in floor heating simulations. Energy and Buildings 2007;39:1107–14.
[13] Laouadi A. Development of a radiant heating and cooling model for building energy simulation software. Building and Environment 2004;39:421–31.
[14] Tu JY, Fuchs L. Calculation of flows using three-dimensional overlapping grids and multigrid methods. International Journal for Numerical Methods in Engineering 1995;38:259–82.
[15] Banks JW, Schwendeman DW, Kapila AK, Henshaw WD. A high-resolution Godunov method for compressible multi-material flow on overlapping grids. Journal of Computational Physics 2007;223:262–97.
[16] Henshaw WD, Chand KK. A composite grid solver for conjugate heat transfer in fluid-structure systems. Journal of Computational Physics 2009;228 (10):3708–41.
[17] Zheng Y, Liou MS. A novel approach of three-dimensional hybrid grid methodology: part 1. Grid generation. Computer Methods in Applied Mechanics and Engineering 2003;192:4147–71.
[18] Desquesnes G, Terracol M, Manoha E, Sagaut P. On the use of a high order overlapping grid method for coupling in CFD/CAA. Journal of Computational Physics 2006;220:355–82.
[19] Chattot JJ, Wang Y. Improved treatment of intersecting bodies with the chimera method and validation with a simple and fast flow solver. Computers & Fluids 1998;27(5–6):721–40.
[20] Neiswanger L, Johnson GA, Carey VP. An experimental study of high Rayleigh number mixed convection in a rectangular enclosure with restricted inlet and outlet openings. Journal of Heat Transfer 1987;109:446–53.
[21] Awbi HB, Hatton A. Mixed convection from heated room surfaces. Energy and Buildings 2000;32:153–66.
[22] Dai GS. Heat transfer. 2nd ed. Beijing: Higher Education Press; 1999.